Journal of Pipeline Science and Engineering 5 (2025) 100256

Contents lists available at ScienceDirect

Journal of Pipeline Science and Engineering

journal homepage: www.keaipublishing.com/en/journals/journal-of-pipeline-science-and-engineering/

Reliability analysis of gas pipelines considering spatial and temporal corrosion variability

Rui Xiao [a,b,*], Tarek Zayed [b], Mohamed A. Meguid [a], Laxmi Sushama [c]

[a] Department of Civil Engineering, McGill University, Montreal, QC H3A 0C3, Canada
[b] Department of Building and Real Estate, The Hong Kong Polytechnic University, Hung Hom, Kowloon, Hong Kong
[c] Department of Civil Engineering, Trottier Institute for Sustainability in Engineering and Design, McGill University, Montreal, QC, Canada

ARTICLE INFO

Keywords:
Gas pipelines
Failure probability
Corrosion
Random field
Spatial and temporal variability

ABSTRACT

The accelerating deterioration rate, notably due to corrosion in buried gas pipelines, has prompted the development of a systematic methodology for assessing structural integrity. This study introduces a methodology to evaluate the system reliability of a corroded gas pipeline, incorporating the spatial and temporal variability in corrosion growth. To capture the spatial variability of the corrosion process, random field theory is applied, which illustrates the correlation between defect depth and length growth, while a stochastic process is utilized to model the temporal evolution of these defects. The methodology considers two primary failure modes, i.e., small leaks and bursts, and investigates how the length scale in random fields, and the correlation strength between these fields influence the failure probability of the pipelines. System reliability is ultimately assessed based on the analysis of individual pipeline segments. The findings underscore the importance of considering spatial variability in estimating the reliability of gas pipelines. The proposed methodology offers a practical and more accurate approach to account for the spatial and temporal dynamics of corrosion, thereby enhancing the accuracy of reliability assessments for corroded gas pipelines.

1. Introduction

Gas pipelines, which include both transmission and distribution networks, are essential components of the global energy infrastructure, enabling the transportation and delivery of natural gas to industrial, commercial, and residential consumers (Salina Farini Bahaman et al., 2024; Khan et al., 2021). As natural gas continues to play a crucial role in the energy mix, particularly in power generation and industrial applications during the transition to a low-carbon economy, the safety and integrity of these pipelines remain of utmost importance. Failures in these systems can lead to catastrophic outcomes such as fires and explosions (Liu and Liang, 2021; Bubbico, 2018). Given that corrosion is a primary cause of pipeline failures (Halim et al., 2020; Shen and Zhou, 2024), developing and implementing a comprehensive integrity management program is imperative. Such a program must accurately evaluate the failure probability and the overall reliability of pipelines susceptible to corrosion, thereby mitigating the risk of corrosion-related incidents and ensuring their safe and reliable operation (Zhang and Zhou, 2022).

Extensive research has been conducted on the reliability analysis of gas pipelines affected by corrosion. This body of research can be divided into several categories, including probabilistic methods, statistical methods (Mahmoud and Dodds, 2022), Bayesian analysis (Yang et al., 2017), and machine learning-based approaches (Mazumder et al., 2021). Probabilistic methods, particularly those including structural reliability techniques, provide valuable insights into failure mechanisms and system uncertainties, enabling a more thorough reliability assessment. Among these methods, Monte Carlo simulation (MCS) is the most commonly applied approach for analyzing the reliability of corroded gas pipelines (Zhou, 2011; Tee and Pesinis, 2017). To improve efficiency, advanced MCS techniques, such as importance sampling (IS) (Gong and Zhou, 2018), Latin hypercube sampling (LHS) (Abyani and Bahaari, 2020), and subset simulation (SS) (Li et al., 2023), have been developed to enhance variance reduction. Additionally, moment methods, including the first-order reliability method (FORM) and the second-order reliability method (SORM) (Gong and Zhou, 2017; Zelmati et al., 2022; Teixeira et al., 2008), are frequently employed. These methods utilize the moments of random variables to approximate the limit state function (LSF) and estimate failure probability.

In the reliability analysis of corroded gas pipelines, two predominant

* Corresponding author.
E-mail address: rui.xiao@mcgill.ca (R. Xiao).

https://doi.org/10.1016/j.jpse.2025.100256
Received 1 August 2024; Received in revised form 23 December 2024; Accepted 6 January 2025
Available online 7 January 2025

failure modes are commonly analyzed: small leaks and bursts. Small leaks occur when corrosion defects fully penetrate the pipeline wall, whereas bursts result from the inability of the remaining strength in the corroded pipeline to withstand the internal pressure (Zhang and Zhou, 2013). Accurately modeling the temporal progression of corrosion defects is essential for reliable pipeline integrity assessments. Research methodologies used to represent corrosion defect growth span a range of approaches, including linear and nonlinear models to random variable approaches and stochastic processes (Bazán and Beck, 2013; Valor et al., 2014; Vanaei et al., 2017). Zhou et al. (2017) employed homogeneous gamma and inverse Gaussian processes to simulate defect growth, using Gaussian copulas to account for dependencies among different defects. They conducted a time-dependent reliability analysis of a pipeline segment using MCS. Chakraborty and Tesfamariam (2021) compared linear growth models and gamma process-based models to assess their impacts on the failure probability of gas pipelines, applying SS to achieve greater accuracy in failure probability calculations. Most studies in this area assume a linear growth in corrosion length over time. Furthermore, the reliability effects of multiple corrosion defects have also been investigated. Abyani and Bahaari (2020) examined the system reliability of pipelines affected by multiple corrosion defects using a series system approach. Wang et al. (2021) developed a framework to assess the reliability of a gas network, modeling it as a series system of pipe segments, where the failure of a segment due to various failure modes was represented using both parallel and series configurations. Furthermore, while the random variables in these analyses are typically considered independent, some studies have explored the impact of their correlations on reliability. These investigations have employed methods such as the Pearson coefficient and copula theory to model the dependencies among variables (Wang et al., 2021; Zhou et al., 2012). This body of research highlights the complexity of accurately predicting pipeline reliability and underscores the importance of utilizing advanced statistical techniques in the field.

The studies reviewed investigated the reliability of corroded gas pipelines by focusing on corrosion defects. In most cases, the prevalence of corrosion was first established before initiating formal analyses. This approach required the identification of the number, location, and parameters of the corrosion defects, as well as their correlation structure. However, the spatial variability in the parameters of the surrounding soil suggests that corrosion defects are likely to exhibit similar variability, which must be incorporated into analyses for more realistic outcomes. Li et al. (2017) and Wang et al. (2021) proposed methodologies to forecast the progression of pitting corrosion on buried ductile pipes by integrating random fields, the gamma process, and copulas. The spatial variability in pipe wall thickness was modeled using a Gaussian random field, while the gamma process described the temporal variability. In a similar vein, Wang et al. (2021) employed a one-dimensional random field to simulate corrosion rates along the pipeline, using the maximum value from a pipeline segment to characterize the corrosion process of that segment.Nahal et al. (2023) introduced a random field to concurrently model the spatial variability of corrosion and residual stress, utilizing the finite element method (FEM) to visualize the impact of corrosion on the structural behavior at each irregular zone. Failure probabilities were evaluated using a series system configuration combined with MCS. While several studies have considered the spatial variability of corrosion in iron pipelines, limited research has focused on its incorporation into the reliability analysis of steel gas pipelines.

Most current studies on the reliability analysis of corroded gas pipelines primarily focus on predefined corrosion defects, often neglecting the influence of spatial variability. While the application of random fields to model corrosion growth has been well-documented for iron water pipes, its utilization in gas pipelines remains relatively limited. Furthermore, many analyses are confined to one-dimensional models that represent corrosion rates only along the depth direction, often disregarding the longitudinal direction. Critically, existing research typically models only the growth of corrosion depth, which directly affects failure probabilities related to minor leaks. However, the residual strength of corroded gas pipelines is influenced by both the depth and length of defects, a fact supported by most relevant standards and codes. Therefore, it is essential to model the growth of corrosion length in reliability analyses. Moreover, given the consistent properties of the surrounding soil at specific pipeline locations, a potential correlation may exist between the growth of corrosion depth and length. Consequently, the relationship between these two random fields requires careful consideration and thorough exploration in the analysis.

This study introduces a methodology to assess the system reliability of corroded gas pipelines. It employs random fields to model the spatial variability in both the depth and length of corrosion, while using a gamma process for modeling temporal variability. LHS is utilized to ensure that the random fields adequately represent all regions of the input space. The analysis considers two failure modes, small leaks and bursts. Additionally, it explores the impact of the random field length scale and the correlation coefficient between the two random fields on the failure probability of gas pipelines. System reliability is evaluated across different pipeline segments. The results offer a practical framework for estimating the reliability of gas pipelines, thereby enhancing integrity management programs, and improving the safety of gas pipelines.

2. Background

2.1. Reliability estimation of corroded gas pipelines

Fig. 1 illustrates a schematic diagram of a corroded gas pipeline segment featuring multiple corrosion defects. The positioning and quantity of these defects are typically determined based on expert knowledge or identified using inline inspection (ILI) technologies such as magnetic flux leakage (MFL) and ultrasonic testing (UT). It is noteworthy that the corrosion surface identified through these technologies often encompasses a cluster of pitting. The diagram specifies the pipeline segment's outside diameter (D), thickness (t), yield strength (σ_y), ultimate tensile strength (σ_u), and the dimensions of each corrosion defect, including depth (d), length (l), and width (w). Generally, two predominant failure modes are observed in gas pipeline incidents: small leaks and bursts. To assess the time-dependent reliability of the pipeline segment under corrosion, the LSF for a small leak at a time τ, which represents a penetrating defect through the pipe wall, is expressed as follows (Xiao et al., 2024; Melchers, 2005):

$$g_l(\tau) = \varphi t - d(\tau) \tag{1}$$

Where φ represents a factor that accounts for the potential development of cracks in the pipe wall, which may lead to leaks in cases of significant corrosion depth; $g_l(\tau)$ denotes the occurrence of a failure resulting from a small leak; $d(\tau)$ represents the depth of the failure.

The burst failure refers to the scenario where the residual strength of a corroded gas pipeline segment is insufficient to withstand the internal pressure, leading to a burst. The LSF for such a burst event at a time τ is expressed as follows (Zhou, 2011; Yu et al., 2021):

$$g_b(\tau) = p_b(\tau) - p_{op}(\tau) \tag{2}$$

Where $p_b(\tau)$ denotes the burst pressure of a corroded pipeline, which is determined by the pipe's geometric and material properties, as well as the characteristics of the corrosion defect; $p_{op}(\tau)$ represents the internal operating pressure of the gas pipeline; and $g_b(\tau)$ indicates the occurrence of a pipeline failure due to a burst.

The parameters considered in this analysis frequently exhibit varying degrees of uncertainty due to factors such as data inaccuracy and model imprecision. These uncertainties are explicitly incorporated by representing as random variables with defined probability distributions. MCS is particularly well-suited for addressing the inherent variability and

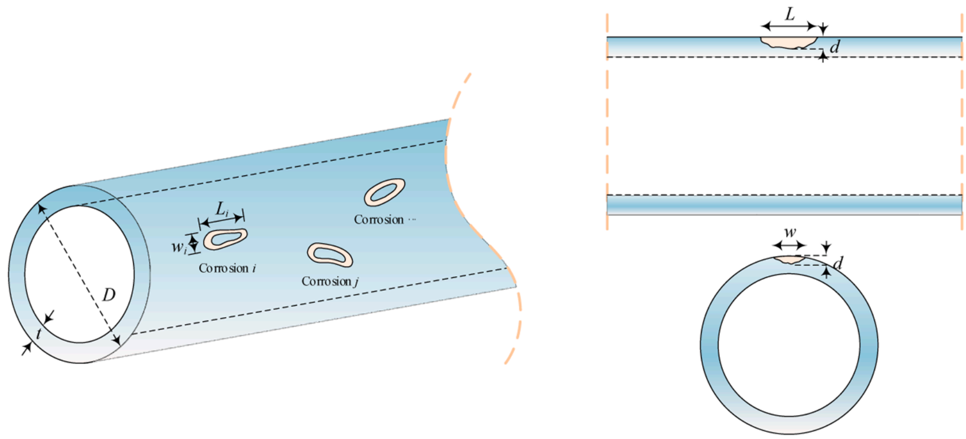

Fig. 1. Schematic diagram of corroded gas pipelines with multiple corrosion defects.

randomness of the system. For a problem involving a set of randomness, denoted by $X = (x_1, \cdots, x_m) \in \mathscr{X} \in \mathbb{R}^m$, where X belongs to a defined value space $\mathscr{X}$, the probability of system failure, P_f, can be generally expressed as follows (Robert and Casella, 2010; Song and Kawai, 2023):

$$P_f = \int_{X \in \mathscr{X}} \mathrm{I}[g(X)] f(X) \mathrm{d}X = \mathbb{E}(\mathrm{I}[g(X)]) \tag{3}$$

Where $\mathrm{I}[\cdot]$ is an indicator function; $g(X)$ represents the LSF encapsulates the system's performance characteristics, as described in Eqs (1) and (2); the failure domain is defined as the set of values of X where $g(X)$ is less than or equal to 0, denoted as $\{X \in \Omega : g(X) \leq 0\}$; $f(X)$ represents the probability density function (PDF) of the random variables X; and $\mathbb{E}$ is the expectation operator with respect to the PDF $f(X)$.

A large number of random samples, adhering to specified probability distributions, are generated and substituted into the LSFs outlined in Eqs (1) and (2). Each sample is evaluated to determine whether the system is in a safe state or has failed. From these evaluations, the probability of failure can be estimated as follows:

$$\widehat{P}_f = \frac{1}{N} \sum_{i=1}^{N} \mathrm{I}[g(X_i)] \tag{4}$$

Where $\{X_i\}_{i \in N}$ denotes a set of independent and identically distributed samples drawn from the distribution $f(X)$; i is the element unit; and N represents the total number of samples.

The variance of $\widehat{P}_f$ and the coefficient of variation (COV) can be further evaluated as follows:

$$\widehat{\sigma}^2_{\widehat{P}_f} = \frac{1}{N} P_f (1 - P_f) \tag{5}$$

$$\mathrm{Cov}_{\widehat{P}_f} = \sqrt{\frac{1 - P_f}{N P_f}} \tag{6}$$

2.2. Random field theory

As discussed in the previous section, assuming specific predefined corrosion defects in estimating the reliability of corroded gas pipelines oversimplifies the issue and overlooks the fact that these pipelines are buried, making them susceptible to spatial variability in soil properties. This context necessitates considering the spatial variability of corrosion defect growth in the modeling process to achieve a more realistic and practical reliability estimation. Such spatial variability can be effectively modeled by random fields, which capture the corrosion process across the entire pipeline surface (Vanmarcke, 2010).

The random field, denoted as $H(\boldsymbol{r}, \omega)$, $\boldsymbol{r} \in \mathscr{D}$, $\omega \in \Omega$ can be considered a generalized stochastic process defined over a topological space $\mathscr{D}$, where $\boldsymbol{r}$ represents a location in space $\mathscr{D}$, ω is an event and Ω is the sample space. This random field provides a mathematical framework for characterizing random variables at any site within the domain $\mathscr{D}$, enabling the modeling of variables that exhibit spatial variability. Such a representation is invaluable in capturing the spatial variability of physical quantities, like the growth of corrosion on a surface, which is appropriately modeled as a continuous random field. In engineering contexts, the stochastic properties of random fields are typically described using the mean μ_H and covariance C_H functions (Christakos, 1992):

$$\mu_H(\boldsymbol{r}) = \mathbb{E}[H(\boldsymbol{r})] = \int_{-\infty}^{\infty} x p_H(x, \boldsymbol{r}) \mathrm{d}x \tag{7}$$

$$C_H(\boldsymbol{r}_i, \boldsymbol{r}_j) = \mathbb{E}\{[H(\boldsymbol{r}_i) - \mu_H(\boldsymbol{r}_i)][H(\boldsymbol{r}_j) - \mu_H(\boldsymbol{r}_j)]\} \tag{8}$$

Where $p_H(x, \boldsymbol{r})$ denotes the PDF of $X(\boldsymbol{r}, \omega)$; $\mu_H(\boldsymbol{r})$ represents the mean value of the random field at a given location $\boldsymbol{r}$; $\boldsymbol{r}_i$ and $\boldsymbol{r}_j$ are two dimensions of the random field; j represents the j-th variable.

To generate realizations of the random field, several commonly used methods can be employed, including the spectral method, turning bands method, and Karhunen-Loève (KL) expansion (Liu et al., 2019). Among these, the KL expansion is particularly favored due to its efficiency in capturing the essential statistical characteristics of the underlying random process using a minimal number of basis functions. Consequently, it is utilized in this study to generate samples of the corrosion growth fields. The KL expansion method decomposes a random right into its eigenvalues λ_i and eigenfunctions $\varphi_i(\boldsymbol{r})$ derived from the covariance matrix. The random field is then discretized using this deterministic set (Betz et al., 2014; Ghanem and Spanos, 1991):

$$H(\boldsymbol{r}, \omega) = H_0(\boldsymbol{r}) + \sum_{i=1}^{\infty} \sqrt{\lambda_i} \xi_i(\omega) \varphi_i(\boldsymbol{r}) \tag{9}$$

Where $H_0(\boldsymbol{r})$ is the mean function of the random field $H(\boldsymbol{r}, \omega)$ and $\xi_i(\omega)$ are standard orthonormal random variables.

The eigenvalues and eigenfunctions of the covariance matrix can be derived by solving the homogeneous Fredholm integral equation (Ghanem and Spanos, 1991):

$$\int_{\Omega} C_H(\boldsymbol{r}_i, \boldsymbol{r}_j) \varphi_i(\boldsymbol{r}_j) \mathrm{d}\boldsymbol{r}_j = \lambda_i \varphi_i(\boldsymbol{r}_i) \tag{10}$$

By determining the covariance function of the random field, the eigenvalues and eigenfunctions can be computed. Using a set of random coefficients $\xi_i(\omega)$ generated from a standard normal distribution and selecting an appropriate number of terms to truncate the expansion, samples of the random field $H(\boldsymbol{r}, \omega)$ can be generated by evaluating the truncated KL expansion at different points in the domain $\mathscr{D}$.

2.3. Latin hypercube sampling (LHS)

LHS is a statistical technique widely used for generating a near-random sample of parameter values from a multidimensional distribution. In this study, it is employed to generate the standard orthonormal random variables $\xi_i(\omega)$ in the KL expansion. A key advantage of LHS is that it ensures the set of random numbers adequately represents real variability, which distinguishes it from traditional random sampling. LHS is based on the principle of stratified sampling, extending this concept to multiple dimensions. Consider a set of variables S_j, $j = 1,2,\cdots,m$, each following a uniform distribution $U(0,1)$. The range $[0,1]$ for each variable is divided into n equally probable, non-overlapping intervals defined as $u_{ij} = [(i-1)/n, i/n)]$, $i = 1,2\cdots,n$. For each interval u_{ij}, a random sample u_{ij}^* is drawn uniformly. To ensure stratification across all dimensions, the order of intervals for each variable is independently permuted, denoted as π_j. The sample $S_j^{(i)}$ for the j-th variable in the i-th sample can be written as (Mckay et al., 2000; Helton and Davis, 2003):

$$S_j^{(i)} = u^*_{\pi_j(i),i}, i = 1,2,\cdots,n \tag{11}$$

This sampling scheme is independent of the number of dimensions, making it suitable for high-dimensional problems. Additionally, LHS allows for the sequential collection of random samples, while ensuring that previously selected samples are tracked. LHS ensures that the set of random numbers represents real variability. Unlike stratified sampling, which is limited to one-dimensional problems, LHS can be applied to multidimensional problems.

3. Reliability analysis of corroded gas pipeline

Fig. 2 provides the general framework followed in this study to estimate the failure probability of the gas pipeline segment and system, which will be detailed in subsequent sections.

3.1. Remaining strength and internal operating pressure models

In order to estimate the reliability of corroded gas pipelines, the LSFs in Eqs. (1) and (2) must be evaluated for each sample. For burst failure, the remaining strength of the corroded gas pipeline, subjected to corrosion defects, to withstand internal pressure needs to be determined. Currently, several engineering standards and codes, such as ASME B31G (ASME, 2012; Zhang et al., 2021), DNV RP-F101 (DNV, 2015), and CSA Z662 (CSA, 2019), have been developed based on full-scale experimental results. The burst pressure p_b in Eq. (12) is a function of pipe geometric and mechanical parameters, such as diameter, thickness, yield strength, and tensile strength, as well as the characteristics of corrosion defects, including defect depth, length, and width. This study utilizes the DNV RP-F101 model to predict the burst pressure due to its superior performance (Bhardwaj et al., 2021; Gong et al., 2024):

$$p_b = 1.05\frac{2\ t}{D-t}\sigma_u\left(\frac{1-d/t}{1-d/t/M}\right) \tag{12}$$

Where M is Folia's bulging factor, and can be expressed as follows:

$$M = \sqrt{1+0.31\left(\frac{L}{\sqrt{Dt}}\right)^2} \tag{13}$$

The internal pressure of an individual gas pipeline is determined according to the design formula for steel pipes outlined in CFR 192.105 and the ASME code for pressure pipelines (ASME, 2014).

$$p_{op} = \frac{2\ \sigma_y t}{D}FET \tag{14}$$

Where F denotes the longitudinal joint factor; E represents the design factor accounting for location class effects; and T is the temperature derating factor that compensates for temperature influences (ASME, 2014).

To accommodate uncertainties and potential fluctuations in demand, a safety factor of 0.72 has been incorporated in the relevant equations to ensure a safety margin. For each sample, the burst pressure of a corroded gas pipeline with specified defect dimensions can be calculated, and the corresponding operating pressure determined. These values are then substituted into the LSF in Eq. (2) to assess whether the pipeline has experienced a burst failure.

3.2. Defect growth model

To estimate the failure probability of a corroded gas pipeline, a more detailed characterization of the defect parameters is required. The

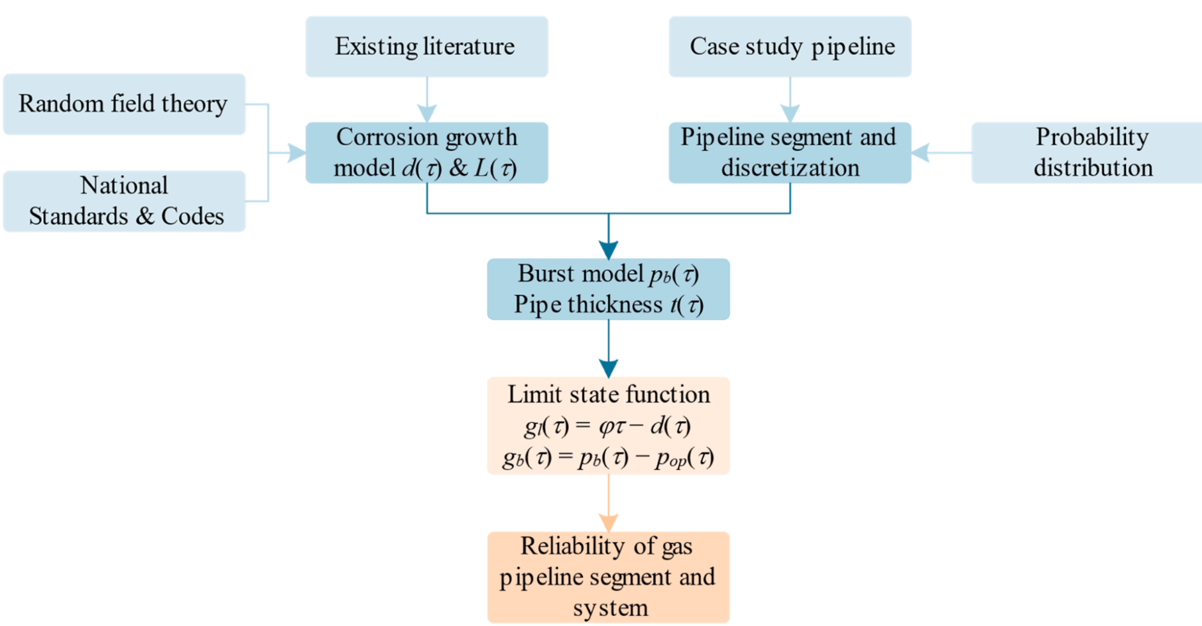

Fig. 2. Framework for reliability analysis of corroded gas pipelines.

progression of corrosion defects is inherently time-dependent, necessitating the prediction of probabilistic distributions for corrosion growth rates. Research has concentrated on developing both linear and nonlinear models to accurately capture this progression. The linear model, which assumes a constant corrosion rate derived from consecutive inspection data, fails to account for the complex characteristics of corrosion processes. Consequently, nonlinear models, particularly the gamma process, have gained traction due to their ability to accurately represent the temporal variability of deterioration. The gamma process is particularly advantageous for stochastic deterioration modeling (Van Noortwijk, 2009; Gong and Zhou, 2018), being positively defined and capable of characterizing the progressive nature of corrosion growth. Therefore, this study employs the gamma process to model defect depth growth, thereby improving the precision of the representation (Van Noortwijk, 2009; Wang et al., 2020)

$$f\left(d_g(\tau)|\alpha(\tau),\beta\right) = \frac{\lambda^{\alpha\tau}}{\Gamma(\alpha\tau)} d_g(\tau)^{\alpha\tau-1} e^{-\beta d_g(\tau)} I_{(0,\infty)}\left[d_g(\tau)\right] \tag{15}$$

Where d_g denotes the depth growth; α and β denote the shape and rate parameters, respectively; and $\Gamma(x) = \int_0^\infty q^{x-1}e^{-q}dq$ is the gamma function where q represents the integration variable and $x > 0$. The mean and variance of a gamma process can be derived as $\alpha(\tau)/\beta$ and $\alpha(\tau)\ /\beta^2$, respectively.

The gamma process exhibits independent increments, where the increment $d_g(\tau + \Delta\tau) - d_g(\tau)$, over the time interval $\Delta\tau$, is distributed as a gamma random variable with shape parameter $\alpha\Delta\tau$ and rate parameter β:

$$d_g(\tau + \Delta\tau) - d_g(\tau) \sim \Gamma(\alpha\Delta\tau, \beta) \tag{16}$$

Thus, the expression for the depth of a single corrosion defect at a time τ is (Jiang et al., 2023):

$$d(\tau) = d_0 + d_g(\tau) \tag{17}$$

Where d_0 is the initial depth of the corrosion defect.

The study utilizes a linear growth model to represent the defect length over time τ. It was found that the impact of corrosion defect length is less significant than that of defect depth. Therefore, a linear growth model was chosen to describe the progression of corrosion length, aligning with established practices in the field (Bazán and Beck, 2013):

$$L(\tau) = L_0 + \dot{L}\tau \tag{18}$$

Where L_0 is the initial defect length and $\dot{L}$ denotes the corrosion rate for defect length.

3.3. Spatial variability depiction

Fig. 3 illustrates the process of unwrapping the curved surface of the pipe and mapping it onto a flat plane. The angular coordinate is mapped linearly to the width of the rectangle, $c = \pi D$, while the longitudinal coordinate z is mapped directly to the length, $l = z$. The spatial variability of the corrosion growth is modeled using a random field. In this study, an exponential decaying covariance function is adopted to describe the spatial correlation between values of the corrosion field at different locations $\boldsymbol{r}_i$ and $\boldsymbol{r}_j$ (Spanos et al., 2007).

$$C_H(\boldsymbol{r}_i, \boldsymbol{r}_j) = \sigma^2 \exp\left(-\frac{\left|(\boldsymbol{r}_i - \boldsymbol{r}_j)_l\right|}{\phi_{lg}} - \frac{\left|(\boldsymbol{r}_i - \boldsymbol{r}_j)_c\right|}{\phi_{cf}}\right) \tag{19}$$

Where σ^2 is the variance; and ϕ_{lg} and ϕ_{cf} are range parameters or length scales in longitudinal and circumferential directions, respectively, controlling the rate of covariance decay with distance.

In disciplines involving random fields, the length scale typically refers to the characteristic distance over which the properties of the random field exhibit significant variation. In the present study, the length scale ϕ characterizes the spatial extent over which the corrosion growth is spatially correlated. A larger value of ϕ indicates a broader spatial correlation, suggesting that corrosion at distant locations is strongly related. Conversely, a smaller value of ϕ implies a more localized correlation, with corrosion growth displaying greater variability over shorter distances. These length scales are typically derived from empirical observations or experimental data, capturing the scale at which the corrosion process exhibits spatial continuity.

Given that corrosion must be modeled as a positive random field, a lognormal random field is employed. A Gaussian random field is initially constructed using the KL expansion approach, where the covariance structure of the corrosion field in Eq. (19) is decomposed into its eigenvalues and eigenfunctions. LHS is then integrated to generate the standard normal variables required in the KL expansion. The Gaussian field can be expressed as a weighted sum of these eigenfunctions with the sampled weights obtained via LHS. The Gaussian field is then exponentiated to transform it into a lognormal random field $H_V(\boldsymbol{r}, \omega)$ with mean μ_V and variance σ_V^2, ensuring all values are positive and capturing the appropriate distribution characteristics of corrosion (Christakos, 1992).

$$H_V(\boldsymbol{r}, \omega) = \exp(\mu_G + \sigma_G H_G(\boldsymbol{r}, \omega)) \tag{20}$$

Where $H_G(\boldsymbol{r}, \omega)$ is the generated Gaussian random field with zero mean and unit variance; and μ_G and σ_G^2 are corresponding normal distribution parameters as given by:

$$\mu_G = \ln\left(\frac{\mu_V^2}{\sqrt{\mu_V^2 + \sigma_V^2}}\right) \tag{21}$$

$$\sigma_G^2 = \ln\left(1 + \frac{\sigma_V^2}{\mu_V^2}\right) \tag{22}$$

The implementation of the random field involves discretizing it at specific points on the pipeline surface. The length L is divided into N_{lg} elements along the longitudinal direction, each with a uniform length $\Delta l = L/N_{lg}$. The width C is divided into N_{cf} elements along the

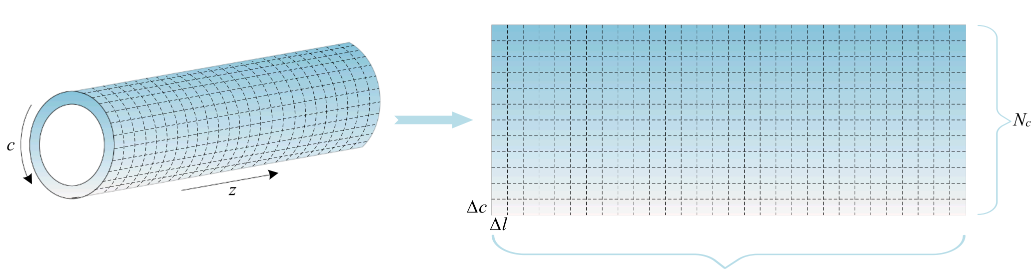

Fig. 3. Illustration of pipeline surface unwrapping and discretization.

circumferential direction, each with a uniform width $\Delta c = \pi D / N_{cf}$. For each element, the average value of the random field at the corners or sampled points within the element is computed and used as the representative value. The number of discretization points should be sufficiently large to accurately approximate the random field. The determination of element size is informed by the progression of corrosion defects that could potentially lead to pipeline failure. This information is derived from field investigations of failed pipelines, including laboratory analyses and failure records maintained by organizations such as PHMSA, ENB, and EGIG. Subsequently, the pipeline diameter is incorporated into the analysis to calculate the discretization number, which is critical for reliability analysis. These considerations form the foundation for the discretization of the pipeline surface in the present study.

For the two corrosion models considered in this study, the shape parameter α is treated as a spatially varying quantity and modeled using a random field to account for the variable corrosion rate across different locations. In contrast, the rate parameter β is fixed to control the overall growth rate of corrosion depth. The corrosion rate $\dot{L}$ in Eq. (18) is also modeled using a random field to account for its spatial variability. By employing this approach, the annual increments of corrosion depth and length can be derived, incorporating spatial variability to assess its impact on the failure probability of gas pipelines.

Corrosion defect growth occurs in both the depth path and the surface direction. Given that the pipeline is exposed to a uniform corrosive soil environment, corrosion development along the depth and length directions is interrelated. This study addresses the correlation between corrosion depth and length using the Nataf transformation, which facilitates modeling the correlation between non-Gaussian random variables. For two lognormal random fields $H_d(\boldsymbol{r}, \omega)$ and $H_l(\boldsymbol{r}, \omega)$, corresponding to corrosion depth and length, with desired correlation ρ_{dl}, the correlation of the corresponding Gaussian fields can be given as (Most, 2005; Ditlevsen and Madsen, 1996):

$$\rho_{G_{dl}} = \frac{\ln(1 + \rho_{dl}\mathrm{COV}_d \cdot \mathrm{COV}_l)}{\sqrt{\ln(1 + \mathrm{COV}_d^2)\ln(1 + \mathrm{COV}_l^2)}} \tag{23}$$

Where COV_d and COV_l are the COVs of $H_d(\boldsymbol{r}, \omega)$ and $H_l(\boldsymbol{r}, \omega)$ respectively.

The Cholesky decomposition is then used to decompose $\rho_{G_{dl}}$ to yield the lower triangular matrix $\boldsymbol{L}$. The Cholesky factor is applied to the generated independent Gaussian random fields to obtain correlated Gaussian random fields. The target lognormal random fields with the desired correlation strength are then obtained by following the procedures outlined in Eqs. (20)–(22).

3.4. Reliability of pipe segment and system

To estimate the failure probability of the gas pipe segment using the proposed methodology, the failure probabilities due to small leaks and burst failures can be determined based on the LSFs in Eqs. (1) and (2). In detail, the corrosion characteristics are quantified for each defect using Eqs. (15)–(18), while the remaining strength of the pipeline is evaluated based on Eqs. (12) and (13), and the operating pressure is calculated using Eq. (14). Parameter uncertainties are represented by random variables, and the spatial variability of the corrosion field is modeled as a random field. The failure probability of the gas pipeline for each failure mode is then estimated using MCS, which involves repeatedly sampling the random variables and random fields and computing the proportion of simulations that lead to pipeline failure as shown in Eq. (4). Notably, as the defect depth increases, the residual strength of the pipeline decreases, potentially increasing the risk of burst failure. This indicates a potential interaction between the small leak and burst failure modes. The composite failure probability for a corroded gas pipeline at a given time τ with a corrosion defect i is defined as follows (Gong and Zhou, 2018; Gong and Zhou, 2017):

$$\begin{aligned} P_{f_i}(\tau) &= P\left(g_{l_i}(\tau) < 0 \cup g_{b_i}(\tau) < 0\right) \\ &= P\left(g_{l_i}(\tau) < 0\right) + P\left(g_{b_i}(\tau) < 0\right) - P\left(g_{l_i}(\tau) < 0 \cap g_{b_i}(\tau) < 0\right) \end{aligned} \tag{24}$$

Considering the spatial variability of the corrosion field, each discretized element of the pipeline surface will experience specific corrosion degradation. For the discretized gas pipeline segment, the failure of any element might lead to the failure of the segment. This problem can be viewed as a subsystem with $N_{lg} \times N_{cf}$ corrosion defects forming a series system, as illustrated in Fig. 3. Therefore, the failure probability of the subsystem can be estimated as (Li and Chen, 2009):

$$P_{f_{sub}}(\tau) = 1 - \prod_{i=1}^{N_l N_c} \left[1 - P_{f_i}(\tau)\right] \tag{25}$$

Based on the topology of the pipeline, it can be classified as a series system, a parallel system, or a mixed system. In a gas pipeline with K multiple segments, a series system indicates that the failure of any individual segment leads to the failure of the entire pipeline. The system failure probability can be estimated as follows:

$$P_{f_{sys}}(\tau) = 1 - \prod_{j=1}^{K} \left[1 - P_{f_{sub_j}}(\tau)\right] \tag{26}$$

For a parallel system, the entire system loses functionality only when all segments fail. The system failure probability for a parallel configuration can be formulated as follows:

$$P_{f_{sys}}(\tau) = \prod_{j=1}^{K} P_{f_{sub_j}}(\tau) \tag{27}$$

In a mixed system, the pipeline consists of both series and parallel subsystems. Calculate each subsystem's failure probability using series and parallel formulas, these probabilities are then combined based on their configuration to determine the overall system failure probability.

In summary, the proposed methodology to estimate the failure probability of corroded gas pipeline segments and the system is outlined in Algorithm 1.

4. Numerical example

This section presents and evaluates the proposed methodology for performing reliability analysis on corroded gas pipeline segments and systems. It includes several examples to illustrate the application of this approach and discusses the resulting findings.

4.1. General information on the pipeline and corrosion process

To demonstrate the procedures and application of the proposed method, case studies are conducted based on a buried steel gas pipeline consisting of ten connected pipeline segments, each measuring 10 m in length. The pipeline is arranged as an interconnected series system to exemplify the proposed methodology in this study. The case study pipeline is made of steel grade API 5L X60, with a diameter of 508 mm and a thickness of 8.74 mm. The yield strength and tensile strength are 413.40 MPa and 516.75 MPa, respectively. The operating pressure is calculated using Eq. (14). Each pipeline segment is divided into elements with specified dimensions $N_{lg} = 100$ in longitudinal and $N_{cf} = 20$ in circumferential directions, resulting in a total of 2,000 elements.

The statistical information on fundamental pipeline parameters and

Algorithm 1
Calculating corrosion-induced failure probabilities in pipeline.

Require:
Given pipeline and discretize it into unit length segments Q_k
Discretize each pipeline segment into elements of dimensions Δl (length) and Δc (circumference)
Given total period T over which the analysis is to be conducted, segmented into years.
Pipeline material and geometrical parameters and corrosion parameter distributions
Number of random samples N
Outputs (Ensure):
Calculate the failure probability of each pipeline segment, and the overall system reliability over the given time span
Steps:
1: Initialize $\tau \leftarrow \tau_0$ (starting time)
2: Discretize pipeline into segments Q_k
3: For each segment Q_k, discretize into $N_l \times N_c$ element units
4: Generate N random samples for pipeline parameters and random fields for the corrosion process
5: Initialize corrosion depth and length $d(\tau_0) \leftarrow d_0$, $L(\tau_0) \leftarrow L_0$ for each sample
6: Calculate the normal operating pressure p_{op} based on Eq. (14) for each sample
7: For $\tau = \tau_0$ to T
8: For each segment Q_k
9: For each element unit i
10: Initialize failure count $N_{k_l} \leftarrow 0$, $N_{k_b} \leftarrow 0$
11: Calculate depth and length increment Δd_i, ΔL_i using the corrosion growth model
12: Update current corrosion depth $d_i(\tau) \leftarrow d_{i_0} + \Delta d_i$ and length $L_i(\tau) \leftarrow L_{i_0} + \Delta L_i$
13: Calculate the remaining strength $P_{b_i}(\tau)$ based on Eq. (12) of the corroded gas pipeline
14: If $g_{l_i}(\tau) = \varphi t - d_i(\tau) < 0$, $N_{k_l} \leftarrow N_{k_l} + 1$ (small leak)
15: If $g_{b_i}(\tau) = p_{b_i}(\tau) - p_{op}(\tau) < 0$, $N_{k_b} \leftarrow N_{k_b} + 1$ (burst)
16: Calculate failure probability $P_{f_{l_i}}(\tau)$ and $P_{f_{b_i}}(\tau)$ due to small leak and burst for segment k in year τ: $P_{f_{l_i}}(\tau) = N_{k_l}/N$, $P_{f_{b_i}}(t) = N_{k_b}/N$, and the composite failure probability based on Eq. (24)
17: Aggregate failure probabilities to calculate subsystem failure probability $P_{f_{sub}}(\tau)$
18: Aggregate failure probabilities to calculate system failure probability $P_{f_{sys}}(\tau)$
19: Increment time $\tau \leftarrow \tau + 1$
20: Return failure probabilities $P_{f_{sub}}(\tau)$ for each segment and the system $P_{f_{sys}}(\tau)$ for each year

the corrosion process is sourced from existing literature and relevant standards. The pipeline diameter, thickness and yield strength are assumed to follow a normal distribution with COV of 0.01, 0.03 and 0.05, respectively. The ultimate tensile strength follows a lognormal distribution with a COV of 0.03, and the operating pressure adheres to a Gumbel distribution with a COV of 0.1. The corrosion process is modeled using random field theory. The initial defect depth and length are assumed to follow a Weibull distribution with a mean of 0.25 mm and a COV of 0.1, and a lognormal distribution with a mean of 50 mm and a COV of 0.1, respectively, uniformly distributed across the entire pipeline surface. The initial corrosion time τ_0 is set at 2.88 years. The growth of the corrosion defect is modeled using a gamma process across the entire pipeline surface. The annual increment follows a gamma distribution with a mean of 0.15 and a COV of 0.2. Similarly, the annual growth of defect length follows a lognormal distribution with a mean of 3 and a COV of 0.2. Considering that the corrosion depth and length at a specific point on the pipeline are influenced by the soil parameters at that location, these dimensions are correlated. Consequently, the covariance function is utilized to model the variability in both corrosion depth and length, with the length scale set uniformly applied in both longitudinal and circumferential directions. The impact of the length scale in the longitudinal and circumferential directions on the failure probability of corroded gas pipelines is investigated in the subsequent analysis. A summary of these parameters' statistics is provided in Table 1.

To perform the reliability analysis, a total of 1×10^6 samples is generated for the pipeline and corrosion parameters following the specified probability distributions. LHS is used to generate the uncorrelated standard normal variables $\xi_i(\omega)$ required to create realizations of the random field. The factor φ in Eq. (1) is set to 0.8 in this study to account for the failure due to small leaks.

4.2. Reliability analysis of gas pipeline segment considering the impact of length scale

This section investigates the impact of the length scale of the random field of corrosion depth and length on the failure probability of a gas pipeline segment. The length scale affects the spatial variability of the random field: shorter lengths result in high variability, while longer lengths lead to smoother transitions. Figs. 4 and 5 present realizations of the random fields for the annual growth of corrosion depth and length, illustrating the influence of length scale on spatial variability, with two distinct length scales, 1 m and 5 m. In Fig. 4, the shorter length scale (1 m) yields a highly irregular and heterogeneous pattern, with rapid variations in corrosion depth increments across both longitudinal and circumferential directions. This indicates frequent changes in corrosion characteristics over short distances. Conversely, with the longer length

Table 1
Statistics of pipeline and corrosion parameters.

Statistics	Pipe diameter (mm) pipeline	Wall thickness (mm)	Yield strength (MPa)	Tensile strength (MPa)	Operating pressure (MPa)	Initial depth (mm) defect	Initial length (mm)	Annual growth depth (mm)	Defect length growth rate (mm/a)
Mean	μ_D	μ_t	μ_{σ_y}	μ_{σ_u}	$\mu_{p_{op}}$	μ_{d_0}	μ_{L_0}	0.15	3.00
COV	0.01	0.03	0.05	0.03	0.10	0.10	0.10	0.20	0.20
Distribution	Normal	Normal	Normal	Lognormal	Gumbel	Weibull	Lognormal	Gamma	Lognormal
Source	Al-Amin and Zhou (2014)	Al-Amin and Zhou (2014)	Al-Amin and Zhou (2014)	Zhou et al. (2017);; Gong and Zhou (2018)	CSA (2019)	Li et al. (2023)	Ben Seghier et al. (2022)	Zhou et al. (2017); Gong and Zhou (2018)	Zhou (2011); Al-Amin and Zhou (2014)

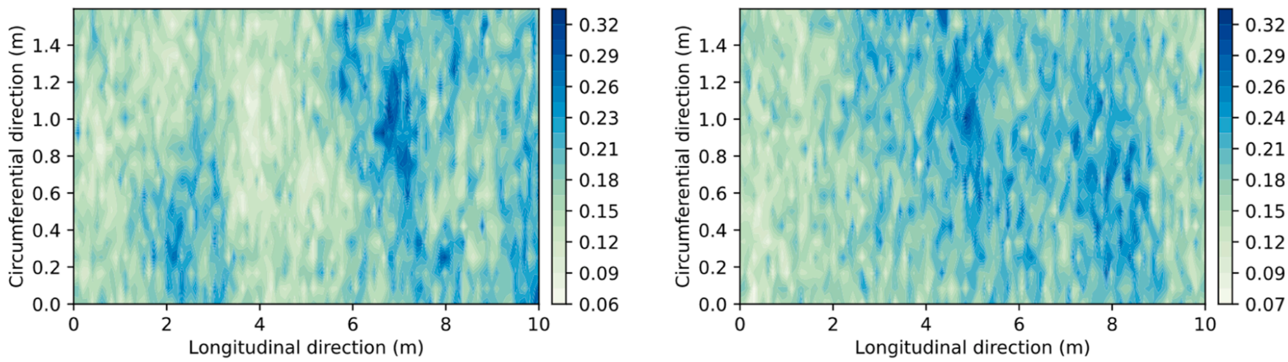

(a) Length scale 1m (b) Length scale 5m

Fig. 4. Realization of random fields for annual corrosion depth increments with varying length scales.

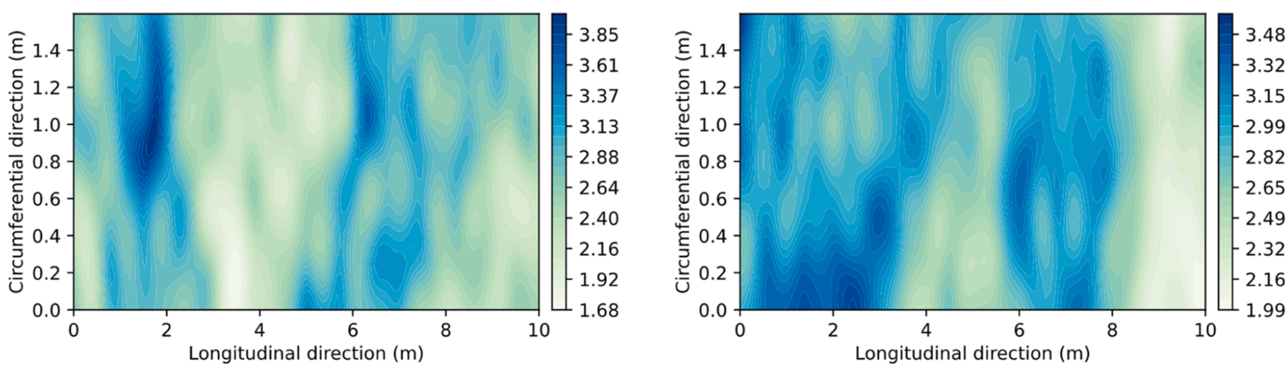

(a) Length scale 1m (b) Length scale 5m

Fig. 5. Realization of random fields for annual corrosion length increments with varying length scales.

scale (5 m), a smoother pattern is observed. Here, the corrosion depth increments change less frequently over larger distances, resulting in a more homogeneous and less intricate spatial structure. A similar pattern is observed in Fig. 5. With a shorter length scale, the random field exhibits significant variability, displaying a complex and finely detailed pattern of corrosion length increments, producing a highly variable and intricate field. In contrast, a longer-length scale displays a smoother and more uniform pattern.

To better illustrate the effect of length scale on the failure probability of corroded gas pipelines, a representative element with a centroid located at (4.950, 0.758) is examined to assess the failure probability of the pipeline segment resulting from these individual corrosion defects. The length scales in the longitudinal and circumferential directions for both corrosion depth and length are set to 0.25 m, 0.5 m, 0.75 m, 1 m, and 1.25 m, while the other direction is fixed at 1 m during the investigation. The correlation coefficient between the two corrosion processes is set at 0.5. The failure probability of the pipeline segment subject to individual corrosion defects with different length scales is presented in Figs. 6 and 7.

The length scale of the random field of corrosion depth affects failure probability, as indicated in Fig. 6. For small leaks, the failure probability increases with a larger length scale when the corrosion period is less than 50 years. Interestingly, this pattern reverses when the time exceeds this critical threshold. Additionally, a diminishing marginal effect is observed with increasing length scale. Similar results are observed for the failure probability of gas pipelines due to bursts. The composite failure probability, calculated based on Eq. (24), is generally higher than that for small leaks and bursts, yet it follows similar patterns. This can be explained by corrosion reliability analysis, a high length scale results in a relatively uniform distribution of corrosion rates, leading to early failures of high-rate points and a higher short-term failure probability. Conversely, a low length scale creates a more heterogeneous distribution, resulting in fewer early failures and a lower short-term failure probability. Over the long term, high length scale scenarios experience early failures of high-rate points, leaving moderate and low-rate points to fail gradually, thus stabilizing the failure probability. In low length scale scenarios, variable corrosion rates cause moderate-rate points to accumulate corrosion depth over time, increasing long-term failure probability. Therefore, after around 50 years, the failure probability in high length scale cases is slightly lower than in low length scale cases.

In contrast, the influence of the length scale of the random field for corrosion length on the failure probability of small leaks and bursts is negligible, as shown in Fig. 7. The failure probability curves for different length scales are nearly identical. This result is intuitive since the failure of small leaks depends on corrosion depth rather than corrosion length. Corrosion depth has a more significant impact on the remaining strength compared to corrosion length, leading to a marginal effect of corrosion length on failure probability. This observation is consistent with findings from previous studies (Bazán and Beck, 2013; Al-Amin and Zhou, 2014).

4.3. Reliability analysis of gas pipeline segment considering the impact of correlation

Fig 8 illustrates the impact of time and positive correlation ($\rho = 0.5$) on the corrosion depth and length of a pipeline continuously exposed to a corrosive environment over periods of 5 and 15 years, displaying random fields for the respective periods. Fig. 8(a) and (b) depict the corrosion depth and length after 5 years. The corrosion depth exhibits moderate spatial variability, indicating localized influences on the pipeline over this period. The corrosion length also shows variability,

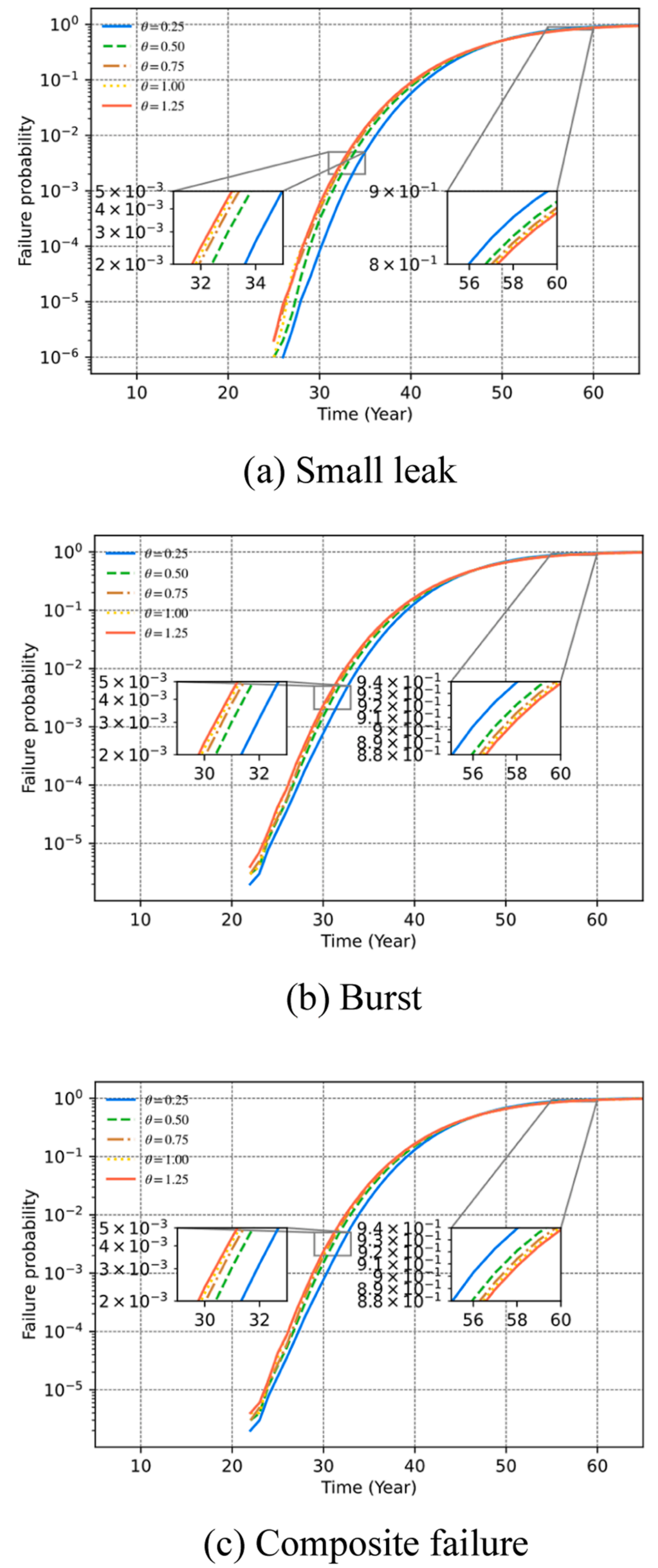

Fig. 6. Failure probability of a pipeline segment with individual corrosion defects, the impact of varying length scales in the random field of corrosion depth.

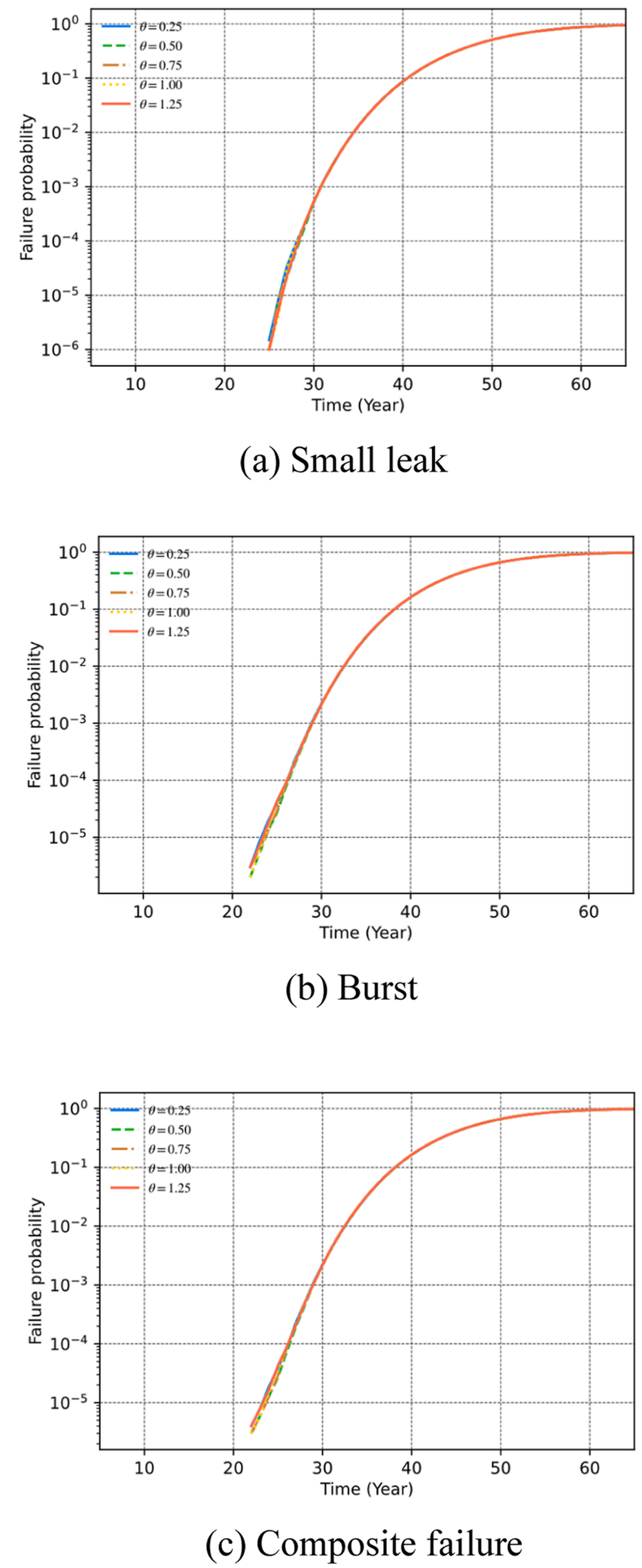

Fig. 7. Failure probability of a pipeline segment with individual corrosion defects, the impact of varying length scales in the random field of corrosion length.

with regions of significant increase. The positive correlation between depth and length results in overlapping patterns, where regions with higher corrosion depth tend to also exhibit greater corrosion length. After 15 years, the corrosion depth shows enhanced spatial variability and more extensive areas of significant corrosion, reflecting prolonged exposure to the environment. Similarly, the corrosion length demonstrates greater variability and smoother transitions. These results underscore the importance of considering both time and correlation in understanding and modeling the long-term corrosion behavior of pipelines.

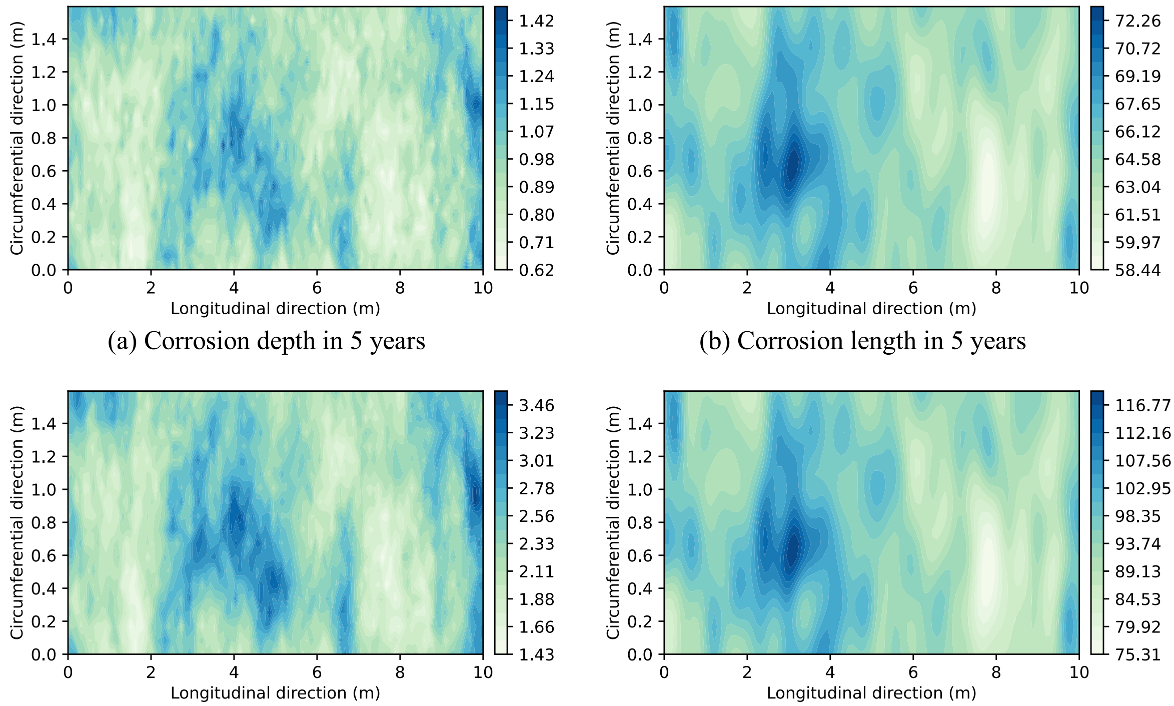

(a) Corrosion depth in 5 years

(b) Corrosion length in 5 years

(c) Corrosion depth in 15 years

(d) Corrosion length in 15 years

Fig. 8. Realization of correlated corrosion depth and length random fields over various periods.

The study further explores the impact of the correlation between corrosion depth and length on the failure probability of gas pipelines. The length scale in both longitudinal and circumferential directions is set to 1 m. Theoretically, a positive correlation indicates a similar growth pattern between corrosion depth and length, thereby increasing the likelihood of failure. This study analyzes five different correlation coefficients: 0.1, 0.3, 0.5, 0.7, and 0.9. The results are illustrated in Fig. 9. It is evident that the correlation of the two random fields has a negligible impact on the failure probability due to small leaks, as corrosion length does not contribute to pipeline failure through perforation. However, it does influence the behavior of burst failures. As the correlation coefficient between the two random fields increases, the failure probability due to burst failures also increases. A more pronounced difference in failure probability is observed before 50 years for burst failures, which reduces over a longer period. This difference also affects the composite failure probability, considering the interaction of small leak and burst failures, as shown in Fig. 9(c). These findings highlight the importance of carefully estimating the correlation between the development of corrosion depth and length when assessing the reliability of gas pipelines, particularly in the early years.

4.4. Subsystem and system reliability

The previous section examined the failure probability of corroded gas pipelines under specified corrosion defects, considering the impact of length scale and correlation coefficients of corrosion fields. This section investigates deeper into the subsystem and system reliability of a gas pipeline segment and the entire pipeline, incorporating both spatial and temporal variability. Initially, a single pipeline segment of ten meters in length is considered, followed by the analysis of the interconnected system. Due to the minimal impact of the length scale of the corrosion length random field on the failure behavior of gas pipelines with individual corrosion defects, this factor is set to 1 m for subsequent analysis. Similarly, the correlation coefficient of the two random fields is set to 0.5 when evaluating the impact of the length scale of the corrosion depth random field, while the length scale of the corrosion depth random field is set to 1 m when investigating the impact of the correlation of the two random fields. For simplicity, the soil properties around the ten segments are assumed to be uniform, and thus the parameters of the corrosion growth models for both corrosion depth and length are the same. This assumption does not affect the results of the current study, as the proposed methodology can be easily extended to a more general case when field inspections provide detailed information about the corrosive parameters of the surrounding soil around the investigated pipeline.

Fig. 10 demonstrates the failure probability of a single pipeline segment due to corrosion, accounting for both spatial and temporal variability. The results are comparable to those shown in Fig. 6, which depicts the failure probability of a pipeline segment with individual corrosion defects. Specifically, an increase in the length scale of the random field for corrosion depth enhances the likelihood of failure at early stages (generally before 35 years) for both small leaks and burst failures. However, this trend reverses over the long term. These findings suggest that the impact of the length scale on the failure probability of a single pipeline segment extends from individual corrosion defects to the entire subsystem. It is also apparent that the failure probability of a pipeline segment, when modeled as a series system incorporating the corrosion process as a random field, is higher than when considering corrosion as individual defects. Consequently, the pipeline segment reaches the end of its service life sooner under this model. This study indicates that a proper treatment of the corrosion process is essential when estimating the reliability of corroded gas pipelines. Simplifying the corrosion into several individual defects underestimates the failure probability. Therefore, it is recommended to use random field theory to accurately account for the spatial variability of the corrosion process, providing a more practical and precise estimation of reliability.

Fig. 11 further investigates the impact of the correlation coefficient

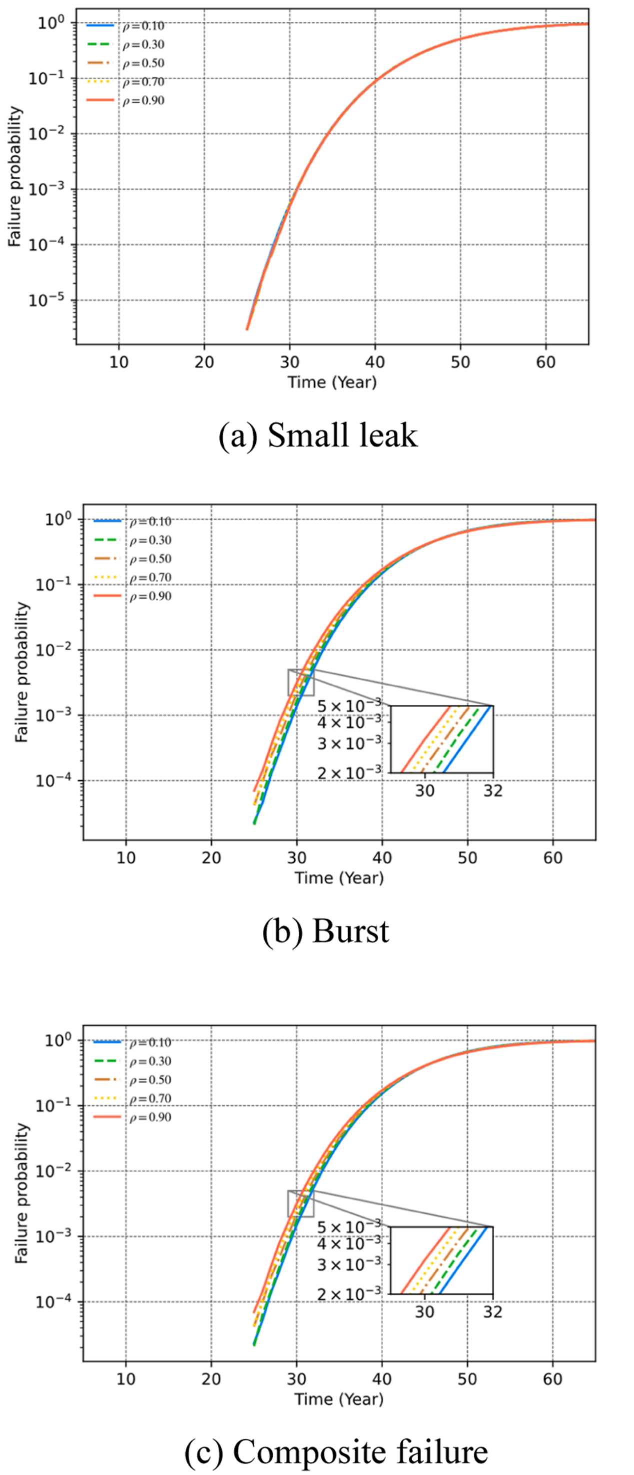

Fig. 9. Failure probability of a pipeline segment with individual corrosion defects, the impact of varying correlation coefficients between corrosion depth and length.

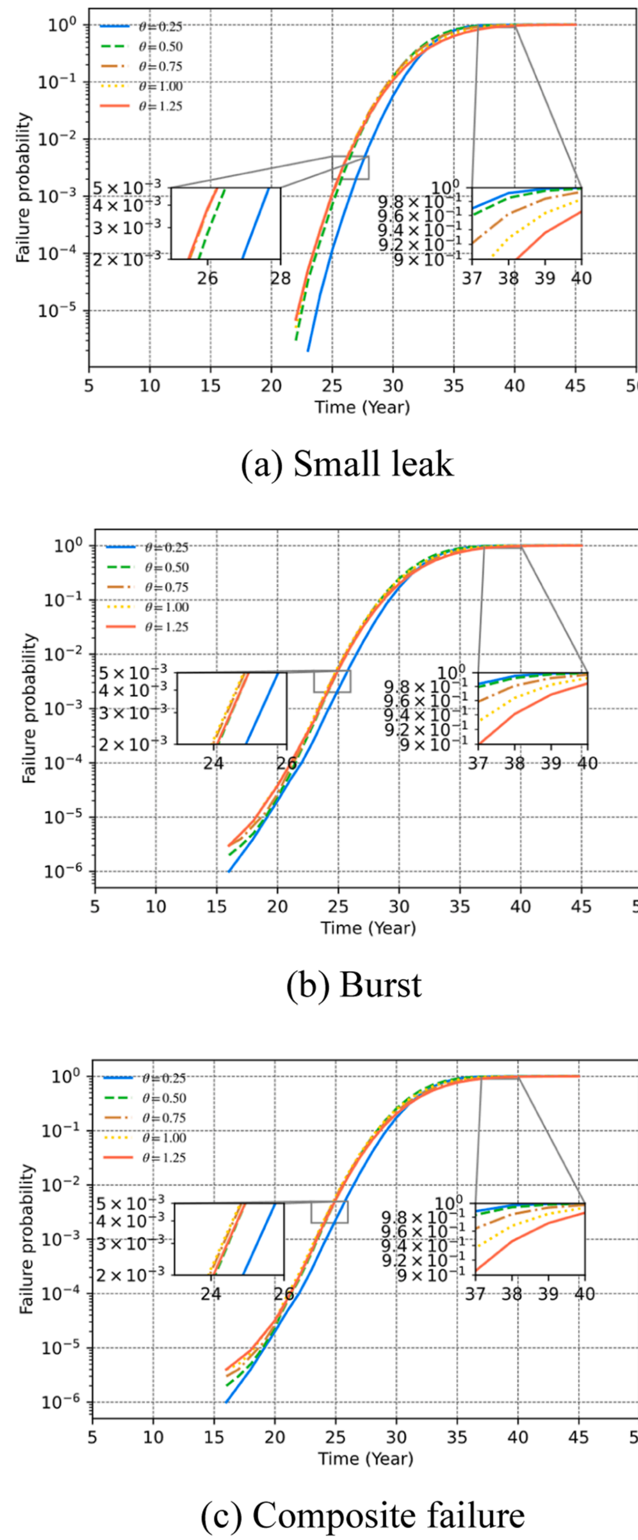

Fig. 10. Failure probability of a pipeline segment due to corrosion considering spatial and temporal variability with the impact of length scale.

between the random fields of corrosion depth and length. The results are similar to those presented in Fig. 7, where the failure probability is estimated based on the corrosion defect level. The correlation between the two random fields has minimal influence on failures due to small leaks, as this failure mechanism is not related to the defect length. However, the correlation does affect burst failures, with a positive correlation increasing the likelihood of failure. This pattern persists from the corrosion defect level to the subsystem level. Similar to the results shown in Fig. 10, the failure probability at the subsystem level is higher than at the corrosion defect level, resulting in the pipeline failing earlier in such scenarios. These findings further emphasize the necessity of modeling corrosion as a random field to accurately assess the reliability of corroded gas pipelines.

The failure probability of the specified gas pipeline is further assessed, with the composite failure probability depicted in Fig. 12.

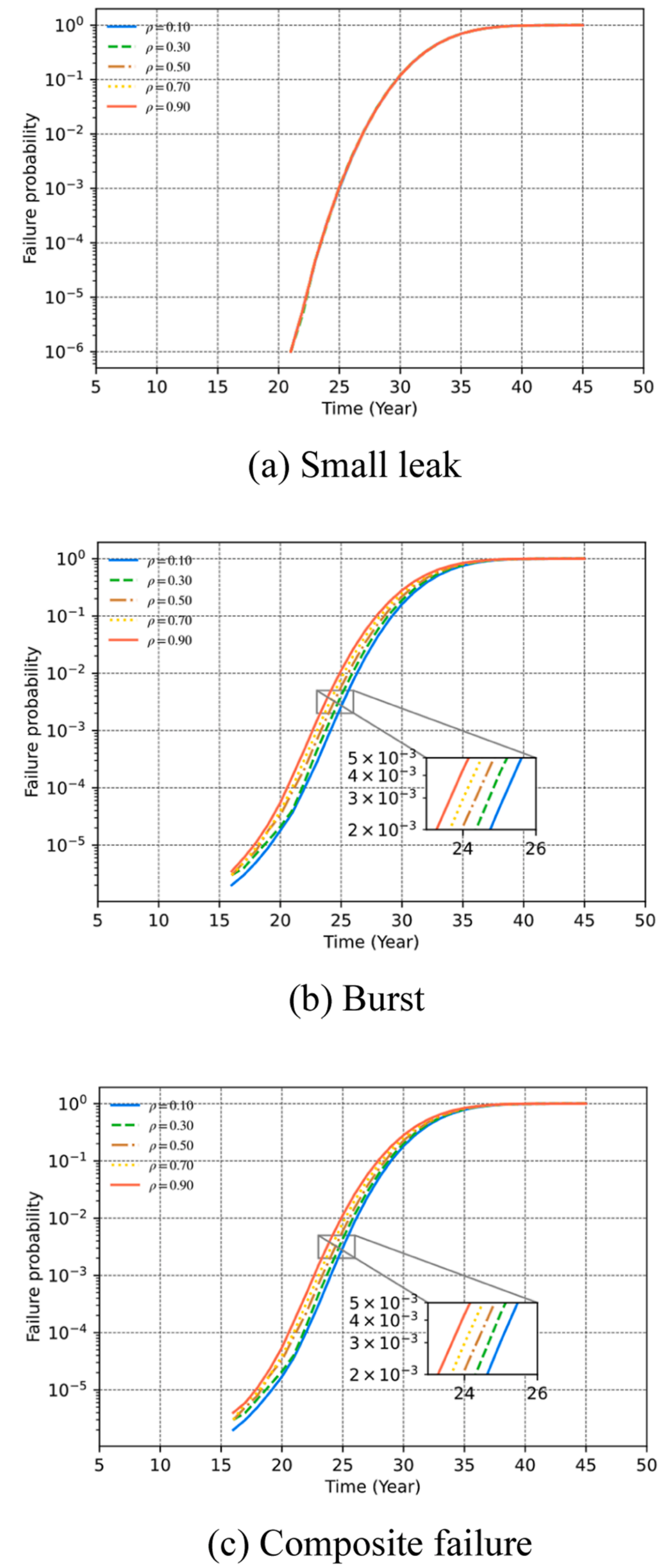

Fig. 11. Failure probability of a pipeline segment due to corrosion considering spatial and temporal variability with the impact of correlation coefficient.

Notably, a similar pattern is observed in Figs. 10 and 11 for subsystems is extended to the composite failure probability of the entire system, which demonstrates higher failure probabilities at the system level. It is important to highlight that this study utilizes a series system for illustrative purposes, although the results for a parallel system could be derived using a similar methodology. For more intricate, mixed systems,

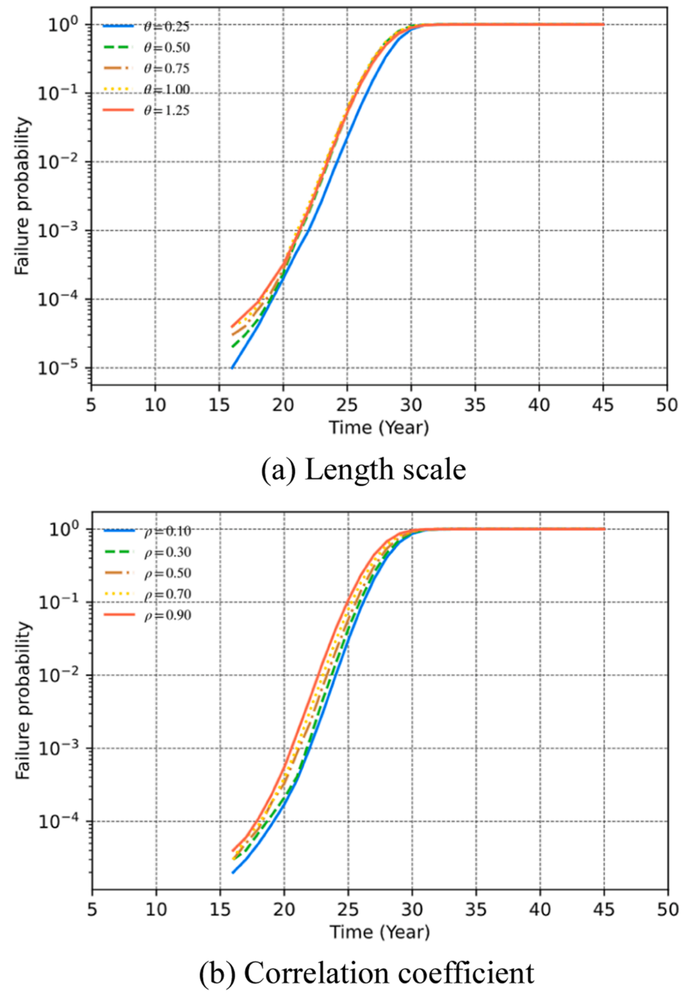

Fig. 12. Failure probability of gas pipelines with the impact of length scale and correlation coefficient.

methods such as the cut set and path set could be employed to identify critical components and facilitate targeted reliability analysis. Overall, the methodology proposed in this study can be generalized to accommodate more complex systems, thereby providing a practical estimation of their failure probabilities.

It is acknowledged that the findings of this study would benefit from further cross-validation using comprehensive field or laboratory datasets, which could provide more practical evidence for the proposed methodology. However, at this stage, such extensive datasets are not available to facilitate this validation. Nonetheless, the MCS method employed in this study offers a robust framework for reliability analysis, as it is well-suited for modeling stochastic failure behaviors in complex systems. Therefore, future research endeavors focus on gathering more extensive datasets to enable thorough cross-validation and enhance the practical applicability of the proposed methodology.

5. Conclusion

This study developed a methodology to estimate the reliability of corroded gas pipelines by considering both the spatial and temporal variability of the corrosion process. The spatial variability of the corrosion field is modeled using random field theory and implemented through the KL expansion approach. LHS was employed to realize the random fields associated with the corrosion process. The growth of corrosion depth is modeled using the gamma process, while the corrosion length was assumed to exhibit a linear behavior over time. The study investigated the impact of the length scale of the random field and the correlation between the two distinct corrosion fields on the failure probability of gas pipelines. Furthermore, the failure behavior of the corroded gas pipeline was analyzed at the defect level, subsystem level and system level. The main findings are summarized as follows.

The length scale of the random field affects the characteristics of the generated random fields. Short length scales result in highly irregular, rapidly varying corrosion patterns, whereas longer length scales produce smoother and more homogeneous patterns. This factor subsequently impacts the failure probability of gas pipelines. A longer length scale of the corrosion depth random field leads to a higher failure risk at early ages, but this trend reverses for long-term observations. In contrast, the length scale of the corrosion length random field has a lesser impact on failure probability. The correlation between the two corrosion fields describing corrosion depth and corrosion length is another important factor influencing pipeline failure. A greater correlation between the two random fields increases the likelihood of burst failures at the corrosion defect, subsystem, and system levels, though it does not significantly affect the likelihood of small leaks. From the defect level to the subsystem and system levels, it is observed that gas pipelines are more likely to fail when corrosion is modeled using a random field that considers both spatial and temporal variability as a whole. This modeling approach highlights that pipelines are likely to reach the end of their service life earlier than expected. This finding suggests the necessity of accounting for both spatial and temporal variability when estimating the reliability of gas pipelines to achieve more accurate and practical results. Such results can then be used to inform comprehensive inspection, maintenance, and repair plans.

It is acknowledged that this study assumed the covariance function of the random field and the correlation between the two random fields. Therefore, it is recommended to incorporate detailed field inspection records that include both corrosion information and the corrosive parameters of the soil surrounding the pipeline. This approach would provide a more refined structure for the random fields, leading to a more accurate reliability estimation. Nevertheless, the current study offers a practical framework to consider the impact of corrosion fields on the reliability of gas pipelines, thereby contributing to improved safety and integrity management of such systems.

CRediT authorship contribution statement

Rui Xiao: Writing – original draft, Validation, Software, Methodology, Conceptualization. **Tarek Zayed:** Writing – review & editing, Supervision, Resources, Methodology, Investigation. **Mohamed A. Meguid:** Writing – review & editing, Supervision, Resources, Investigation. **Laxmi Sushama:** Writing – review & editing, Supervision, Resources, Investigation.

Declaration of competing interest

The authors declare that they have no known competing financial interests or personal relationships that could have appeared to influence the work reported in this paper.

Acknowledgments

The first author gratefully acknowledges the support received from The Hong Kong Polytechnic University and McGill University through the Joint Postdoc Scheme.

References

Abyani, M., Bahaari, M.R., 2020. A comparative reliability study of corroded pipelines based on Monte Carlo simulation and latin hypercube sampling methods. Int. J. Press. Vess. Piping 181, 104079. https://doi.org/10.1016/j.ijpvp.2020.104079.

Al-Amin, M., Zhou, W., 2014. Evaluating the system reliability of corroding pipelines based on inspection data. Struc. Infrastruc. Eng. 10, 1161–1175. https://doi.org/10.1080/15732479.2013.793725.

ASME, 2012. ASME B31G-2012: Manual for determining the remaining strength of corroded pipelines: a supplement to ASME B31 code for pressure piping: an American National Standard. Revision of ASME B31G-2009. American Society of Mechanical Engineers, New York, N.Y.

ASME, 2014. ASME - B31.8, Gas Transmission and Distribution Piping Systems. ASME Code for Pressure Piping, B31. The American Society of Mechanical Engineers, New York.

Bazán, F.A.V., Beck, A.T., 2013. Stochastic process corrosion growth models for pipeline reliability. Corros. Sci. 74, 50–58. https://doi.org/10.1016/j.corsci.2013.04.011.

Ben Seghier, M.E.A., Mustaffa, Z., Zayed, T., 2022. Reliability assessment of subsea pipelines under the effect of spanning load and corrosion degradation. J. Nat. Gas. Sci. Eng. 102, 104569. https://doi.org/10.1016/j.jngse.2022.104569.

Betz, W., Papaioannou, I., Straub, D., 2014. Numerical methods for the discretization of random fields by means of the Karhunen–Loève expansion. Comput. Methods Appl. Mech. Eng. 271, 109–129. https://doi.org/10.1016/j.cma.2013.12.010.

Bhardwaj, U., Teixeira, A.P., Guedes Soares, C., 2021. Burst strength assessment of X100 to X120 ultra-high strength corroded pipes. Ocean Eng. 241, 110004. https://doi.org/10.1016/j.oceaneng.2021.110004.

Bubbico, R., 2018. A statistical analysis of causes and consequences of the release of hazardous materials from pipelines. The influence of layout. J. Loss. Prev. Process. Ind. 56, 458–466. https://doi.org/10.1016/j.jlp.2018.10.006.

Chakraborty, S., Tesfamariam, S., 2021. Subset simulation based approach for space-time-dependent system reliability analysis of corroding pipelines. Struc. Saf. 90, 102073. https://doi.org/10.1016/j.strusafe.2020.102073.

Christakos, G., 1992. Random field models in earth sciences. Academic Press, San Diego.

CSA, 2019. Z662:19, Oil and gas pipeline systems. CSA Group.

Ditlevsen, O., Madsen, H.O., 1996. Structural reliability methods. Wiley, Chichester; New York.

DNV, 2015. DNV-RP-F101, Corroded pipelines.

Ghanem, R., Spanos, P.D., 1991. Stochastic finite elements: a spectral approach. Springer-Verlag, New York.

Gong, C., Zhou, W., 2017. First-order reliability method-based system reliability analyses of corroding pipelines considering multiple defects and failure modes. Struc. Infrastruc. Eng. 13, 1451–1461. https://doi.org/10.1080/15732479.2017.1285330.

Gong, C., Zhou, W., 2018. Importance sampling-based system reliability analysis of corroding pipelines considering multiple failure modes. Reliab. Eng. Syst. Saf. 169, 199–208. https://doi.org/10.1016/j.ress.2017.08.023.

Gong, C., Zhou, W., 2018. Importance sampling-based system reliability analysis of corroding pipelines considering multiple failure modes. Reliab. Eng. Syst. Saf. 169, 199–208. https://doi.org/10.1016/j.ress.2017.08.023.

Gong, C., Guo, S., Zhang, R., Frangopol, D.M., 2024. Prediction of burst pressure of corroded thin-walled pipeline elbows subjected to internal pressure. Thin-Walled Struc. 199, 111861. https://doi.org/10.1016/j.tws.2024.111861.

Halim, S.Z., Yu, M., Escobar, H., Quddus, N., 2020. Towards a causal model from pipeline incident data analysis. Proc. Saf. Environ. Prot. 143, 348–360. https://doi.org/10.1016/j.psep.2020.06.047.

Helton, J.C., Davis, F.J., 2003. Latin hypercube sampling and the propagation of uncertainty in analyses of complex systems. Reliab. Eng. Syst. Saf. 81, 23–69. https://doi.org/10.1016/S0951-8320(03)00058-9.

Jiang, F., Dong, S., Zhao, E., 2023. A study on burst failure mechanism analysis and quantitative risk assessment of corroded pipelines with random pitting clusters. Ocean Eng. 284, 115258. https://doi.org/10.1016/j.oceaneng.2023.115258.

Khan, F., Yarveisy, R., Abbassi, R., 2021. Risk-based pipeline integrity management: a road map for the resilient pipelines. J. Pipeline Sci. Eng. 1, 74–87. https://doi.org/10.1016/j.jpse.2021.02.001.

Li, J., Chen, J., 2009. Stochastic dynamics of structures. Wiley, Singapore.

Li, C-Q, Firouzi, A., Yang, W., 2017. Prediction of pitting corrosion–Induced perforation of ductile iron pipes. J. Eng. Mech. 143, 04017048. https://doi.org/10.1061/(ASCE)EM.1943-7889.0001258.

Li, C., Yang, F., Jia, W., Liu, C., Zeng, J., Song, S., et al., 2023. Pipelines reliability assessment considering corrosion-related failure modes and probability distributions characteristic using subset simulation. Proc. Safety Environ. Protec. 178, 226–239. https://doi.org/10.1016/j.psep.2023.08.013.

Liu, S., Liang, Y., 2021. Statistics of catastrophic hazardous liquid pipeline accidents. Reliab. Eng. Syst. Saf. 208, 107389. https://doi.org/10.1016/j.ress.2020.107389.

Liu, Y., Li, J., Sun, S., Yu, B., 2019. Advances in Gaussian random field generation: a review. Comput. Geosci. 23, 1011–1047. https://doi.org/10.1007/s10596-019-09867-y.

Mahmoud, R.M.A., Dodds, P.E., 2022. A technical evaluation to analyse of potential repurposing of submarine pipelines for hydrogen and CCS using survival analysis. Ocean Eng. 266, 112893. https://doi.org/10.1016/j.oceaneng.2022.112893.

Mazumder, R.K., Salman, A.M., Li, Y., 2021. Failure risk analysis of pipelines using data-driven machine learning algorithms. Struc. Saf. 89, 102047. https://doi.org/10.1016/j.strusafe.2020.102047.

Mckay, M.D., Beckman, R.J., Conover, W.J., 2000. A comparison of three methods for selecting values of input variables in the analysis of output from a computer code. Technometrics 42, 55–61. https://doi.org/10.1080/00401706.2000.10485979.

Melchers, R.E., 2005. The effect of corrosion on the structural reliability of steel offshore structures. Corros. Sci. 47, 2391–2410. https://doi.org/10.1016/j.corsci.2005.04.004.

Most, T., 2005. Stochastic crack growth simulation in reinforced concrete structures by means of coupled finite element and meshless methods. https://doi.org/10.13140/2.1.4815.8407.

Nahal, M., Sahraoui, Y., Khelif, R., Chateauneuf, A., 2023. System reliability of corroded pipelines considering spatial and stochastic dependency in irregular zones. Gas Sci. Eng. 117, 205083. https://doi.org/10.1016/j.jgsce.2023.205083.

Robert, C.P., Casella, G., 2010. Monte Carlo statistical methods, 2nd ed. Springer, New York, NY https://doi.org/10.1007/978-1-4757-4145-2.

Salina Farini Bahaman, U., Mustaffa, Z., Ben Seghier, M.E.A., Badri, T.M., 2024. Evaluating the reliability and integrity of composite pipelines in the oil and gas sector: a scientometric and systematic analysis. Ocean Eng. 303, 117773. https://doi.org/10.1016/j.oceaneng.2024.117773.

Shen, Y., Zhou, W., 2024. A comparison of onshore oil and gas transmission pipeline incident statistics in Canada and the United States. Int. J. Crit. Infrastruc. Prot. 45, 100679. https://doi.org/10.1016/j.ijcip.2024.100679.

Song, C., Kawai, R., 2023. Monte Carlo and variance reduction methods for structural reliability analysis: a comprehensive review. Probab. Eng. Mech. 73, 103479. https://doi.org/10.1016/j.probengmech.2023.103479.

Spanos, P.D., Beer, M., Red-Horse, J., 2007. Karhunen–Loéve expansion of stochastic processes with a modified exponential covariance kernel. J. Eng. Mech. 133, 773–779. https://doi.org/10.1061/(ASCE)0733-9399(2007)133:7(773).

Tee, K.F., Pesinis, K., 2017. Reliability prediction for corroding natural gas pipelines. Tunnel. Undergr. Space Technol. 65, 91–105. https://doi.org/10.1016/j.tust.2017.02.009.

Teixeira, A.P., Guedes Soares, C., Netto, T.A., Estefen, S.F., 2008. Reliability of pipelines with corrosion defects. Int. J. Press. Vess. Piping 85, 228–237. https://doi.org/10.1016/j.ijpvp.2007.09.002.

Valor, A., Caleyo, F., Alfonso, L., Vidal, J., Hallen, J.M., 2014. Statistical analysis of pitting corrosion field data and their use for realistic reliability estimations in non-piggable pipeline systems. CORROSION 70, 1090–1100. https://doi.org/10.5006/1195.

Van Noortwijk, J.M., 2009. A survey of the application of gamma processes in maintenance. Reliab. Eng. Syst. Saf. 94, 2–21. https://doi.org/10.1016/j.ress.2007.03.019.

Vanaei, H.R., Eslami, A., Egbewande, A., 2017. A review on pipeline corrosion, in-line inspection (ILI), and corrosion growth rate models. International Journal of Pressure Vessels and Piping 149, 43–54. https://doi.org/10.1016/j.ijpvp.2016.11.007.

Vanmarcke, E., 2010. Random fields: analysis and synthesis, Rev. and expanded new ed. World Scientific, New Jersey.

Wang, Y., Dann, M.R., Zhang, P., 2020. Reliability analysis of corroded pipelines considering 3D defect growth. Thin-Walled Struc. 157, 107028. https://doi.org/10.1016/j.tws.2020.107028.

Wang, W., Wang, Y., Zhang, B., Shi, W., Li, C.Q., 2021. Failure prediction of buried pipe network with multiple failure modes and spatial randomness of corrosion. Int. J. Press. Vess. Piping 191, 104367. https://doi.org/10.1016/j.ijpvp.2021.104367.

Wang, W., Yang, W., Shi, W., Li, C.Q., 2021. Modeling of Corrosion Pit Growth for Buried Pipeline Considering Spatial and Temporal Variability. J. Eng. Mech. 147, 04021065. https://doi.org/10.1061/(ASCE)EM.1943-7889.0001957.

Xiao, R., Zayed, T., Meguid, M.A, Sushama, L., 2024. Time varying reliability analysis of corroded gas pipelines using copula and importance sampling. Ocean Eng. 306, 118086. https://doi.org/10.1016/j.oceaneng.2024.118086.

Yang, Y., Khan, F., Thodi, P., Abbassi, R., 2017. Corrosion induced failure analysis of subsea pipelines. Reliab. Eng. Syst. Saf. 159, 214–222. https://doi.org/10.1016/j.ress.2016.11.014.

Yu, W., Huang, W., Wen, K., Zhang, J., Liu, H., Wang, K., et al., 2021. Subset simulation-based reliability analysis of the corroding natural gas pipeline. Reliab. Eng. Syst. Saf. 213, 107661. https://doi.org/10.1016/j.ress.2021.107661.

Zelmati, D., Bouledroua, O., Ghelloudj, O., Amirat, A., Djukic, M.B., 2022. A probabilistic approach to estimate the remaining life and reliability of corroded pipelines. J. Nat. Gas. Sci. Eng. 99, 104387. https://doi.org/10.1016/j.jngse.2021.104387.

Zhang, S., Zhou, W., 2013. System reliability of corroding pipelines considering stochastic process-based models for defect growth and internal pressure. Int. J. Press. Vess. Piping 111–112, 120–130. https://doi.org/10.1016/j.ijpvp.2013.06.002.

Zhang, S., Zhou, W., 2022. Assessment of the interaction of corrosion defects on steel pipelines under combined internal pressure and longitudinal compression using finite element analysis. Thin-Walled Struc. 171, 108771. https://doi.org/10.1016/j.tws.2021.108771.

Zhang, Z., Guo, L., Cheng, Y.F., 2021. Interaction between internal and external defects on pipelines and its effect on failure pressure. Thin-Walled Struc. 159, 107230. https://doi.org/10.1016/j.tws.2020.107230.

Zhou, W., Hong, H.P., Zhang, S., 2012. Impact of dependent stochastic defect growth on system reliability of corroding pipelines. Int. J. Press. Vess. Piping 96–97, 68–77. https://doi.org/10.1016/j.ijpvp.2012.06.005.

Zhou, W., Xiang, W., Hong, H.P., 2017. Sensitivity of system reliability of corroding pipelines to modeling of stochastic growth of corrosion defects. Reliab. Eng. Syst. Saf. 167, 428–438. https://doi.org/10.1016/j.ress.2017.06.025.

Zhou, W., 2011. Reliability evaluation of corroding pipelines considering multiple failure modes and time-dependent internal pressure. J. Infrastruct. Syst. 17, 216–224. https://doi.org/10.1061/(ASCE)IS.1943-555X.0000063.